Supporting Information

to

True ferroelectric switching in thin films of trialkylbenzene-1,3,5-tricarboxamide (BTA)

A. V. Gorbunov[1], T. Putzeys[2], I. Urbanavičiūtė[3], R.A.J. Janssen[1], M. Wübbenhorst[2], R. P. Sijbesma[4], M. Kemerink[1,3]

[1] Department of Applied Physics, Eindhoven University of Technology, PO Box 513, 5600 MB Eindhoven, The Netherlands

[2] Department of Physics and Astronomy, Laboratory for Soft Matter and Biophysics, KU Leuven, Celestijnenlaan 200D, B-3001 Heverlee, Belgium

[3] Complex Materials and Devices, Department of Physics, Chemistry and Biology (IFM), Linköping University, 58183 Linköping, Sweden

[4] Laboratory of Macromolecular and Organic Chemistry, Eindhoven University of Technology, P.O. Box 513, 5600 MB Eindhoven, The Netherlands

Contents

1 – Differential Scanning Calorimetry

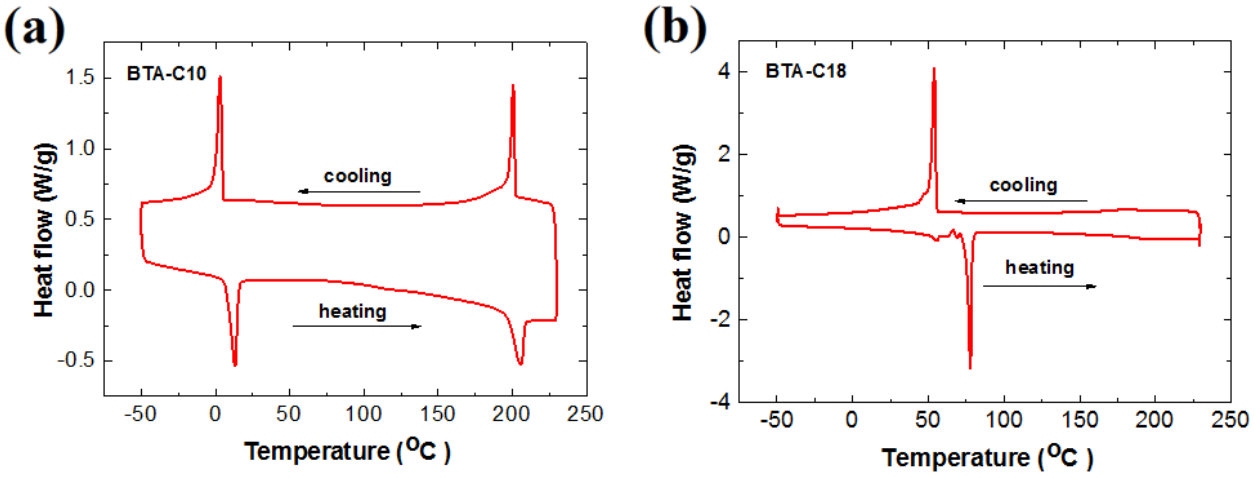

Fig. S1. Differential scanning calorimetry (DSC) traces of BTA-C10 (a) and BTA-C18 (b) obtained at the 2nd cycle. BTA-C10 (BTA-C18) has a crystalline phase below 12 (69) °C, followed by a columnar hexagonal liquid crystalline phase till 200 (~190) °C, after which an isotropic molten phase follows. See also Ref. [1]

Differential Scanning Calorimetry (DSC) studies were performed in hermetic T-zero aluminum sample pans using a TA Instruments Q2000 – 1037 DSC equipped with a RCS90 cooling accessory. The thermal transitions were studied mainly on the second ramps with a rate of 10° C/min.

2 - Polarization optical microscopy

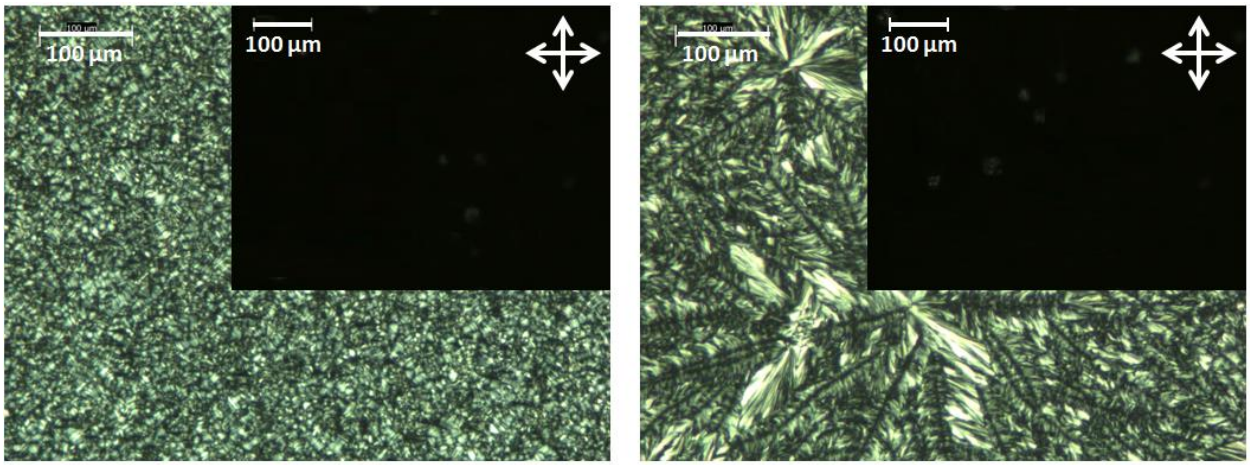

Fig. S2. High resolution polarization optical microscopic (POM) images in cross-polarized light of non-aligned and aligned BTA-C18 (left) and BTA-C10 materials (right), respectively. All images were obtained from transparent liquid crystal cell devices with a 5 µm gap.

Polarized optical microscopy (POM) was performed on a Leica CTR 6000 microscope equipped with two crossed polarizers, a Linkam hot-stage THMS600 as sample holder, a Linkam TMS94 controller and a Leica DFC420 C camera.

For the preparation of liquid crystal (LC) cell devices for optical microscopy experiments, we used transparent commercial LCC5 Linkam cells with 5 µm in gap and 0.81 cm^2 in area. LC cells were filled due to capillary forces from the isotropic melt of BTAs achieved by heating up to 210-230 °C.

3 – X-ray diffraction

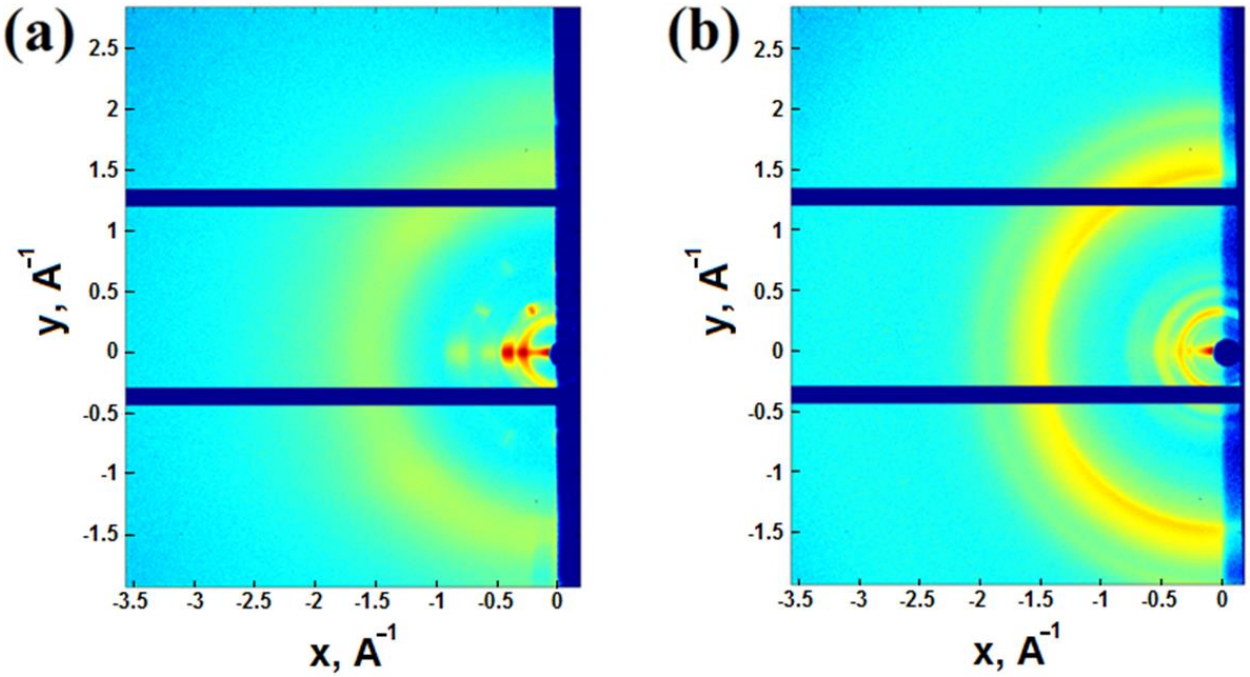

Fig. S3 GIWAXS data on spin-coated thin films of BTA-C10 (a, 0-18°) and BTA-C18 (b, 0-14°) obtained at room temperature showing a hexagonal crystal structure.

The X-ray scattering pattern of BTA-C10 and BTA-C18 at 80 °C is shown in Fig. S3. In the small angle regime of BTA-C10 there are three distinct equatorial reflection peaks at 3.24 nm^{-1}, 5.63 nm^{-1} and 6.48 nm^{-1}, corresponding to the lattice distances d[100] = 1.94 nm, d[110] = 1.12 nm and d[200] = 0.97 nm, respectively. The reciprocal spacing ratio of 1:√3:2 in q-space of these three peaks was assigned to a hexagonal columnar mesophase. In the wide angle regime, the broad diffuse halo corresponds to the liquid-like alkyl chains and the reflection at 17.81 nm^{-1}, with a d spacing of 0.35 nm, has a value typical of the inter-discotic distance of ordered BTAs. The more disordered nature of BTA-C18 prevented an accurate parameter extraction.

X-Ray Diffraction (XRD) images were recorded on a Ganesha lab instrument equipped with a Genix-Cu ultra-low divergence source producing X-ray photons with a wavelength of 1.54 Å and a flux of 1×10^8 photons/second. Diffraction patterns were collected on a Pilatus 300K detector with reversed-biased silicon diode array sensor. The detector consists out of three plates with a 17 pixels spacing in between, resulting in two dark bands on the image. Gracing Incidence X-Ray Scattering (GIXS) measurements were performed on a sample to detector distance of 1080 mm (WAXS). Azimuthal integration of the obtained diffraction patterns was performed by utilizing the SAXSGUI software.

4 –DRS loss spectra + relaxations

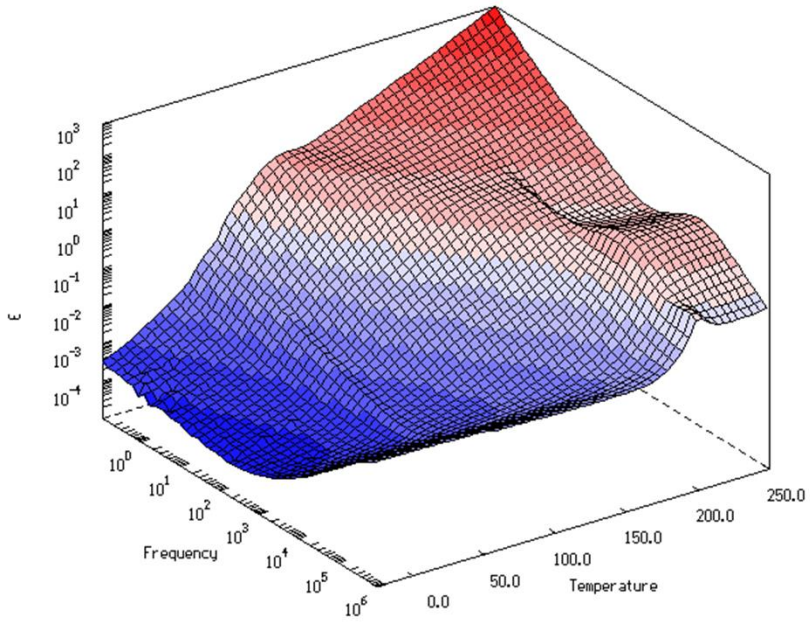

Fig. S4. Dielectric loss ε''(*f*, *T*) for BTA-C18 measured upon cooling from 250°C to 25°C.

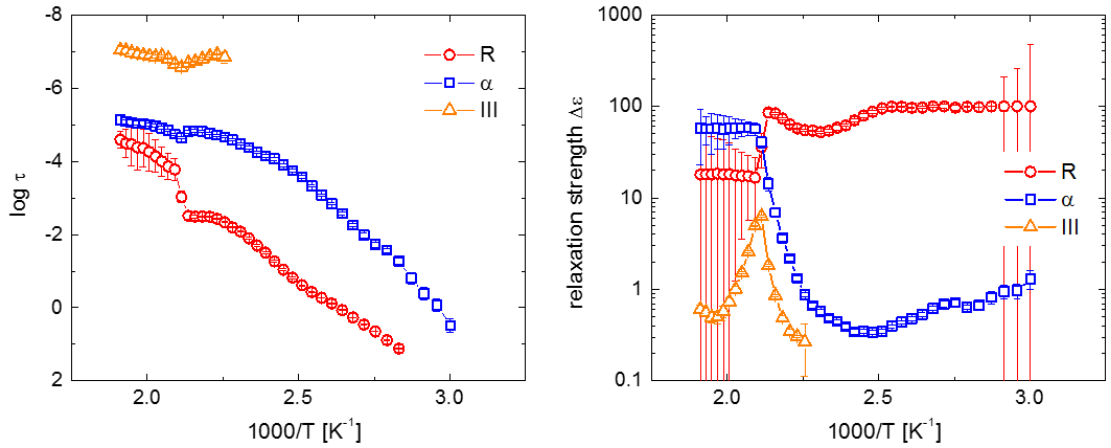

Fig. S5. Relaxation time and strength for BTA-C18 measured upon cooling from 250 °C to 25 °C. *R*- and α-relaxations (red and blue symbols, respectively) are complementary, as shown by the crossing of the corresponding relaxation strengths at the paraelectric to ferroelectric phase transition at 1000/*T* ≈ 2.11 (≈ 200 °C). At the same temperature the strength of the fast III-relaxation peaks, proving that this is a transitional phenomenon giving rise to the observed Curie-Weiss behavior.

The parameters in Fig. S4 were obtained by simultaneous fitting of 2 Cole-Cole functions (for *R*- and α-relaxation) and 1 Debye-relaxation (for process III) to either ε'' or dε'/d(ln(f)) spectra. Both fits led to identical results. The relaxation strength $\Delta\varepsilon$ is defined as the difference between ε' at frequencies far above and far below the reciprocal relaxation time. The fitting procedures are described in detail in Refs. [2,3].

5 – Non-saturated and dynamic polarization loops

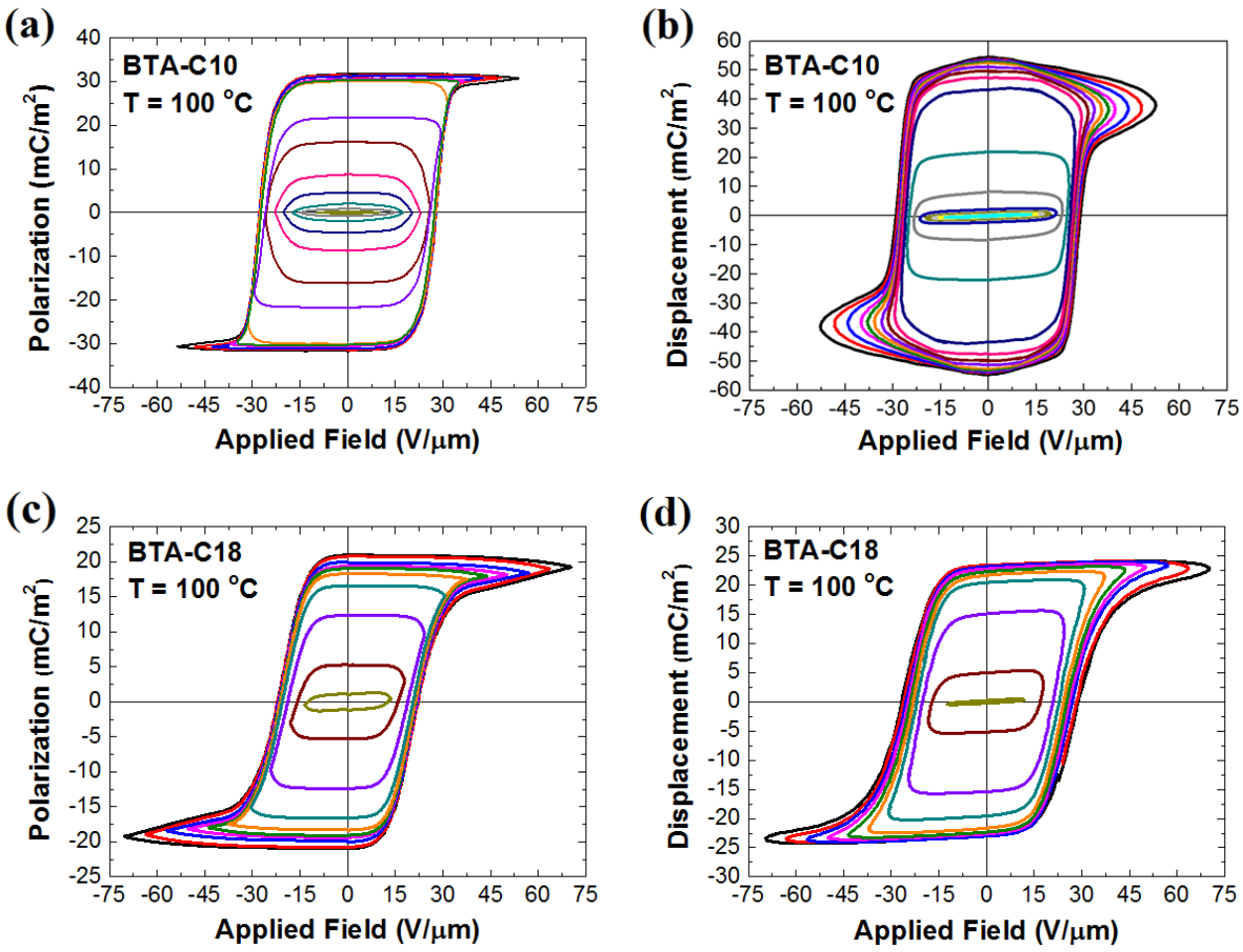

Fig. S6. Saturated and non-saturated polarization loops for BTA-C10 (a,b) and BTA-C18 (c,d) measured quasi-statically (a,c) and dynamically (b,d). Quasi-static and dynamic mode measurements are taken at a frequency of 1 Hz respectively 15 Hz.

The non-ideal shape of the hysteresis loops in Figs. S6(b,d) is a consequence of the fact that these are measured in dynamic mode without subtraction of the background signal as is done in the quasi-static measurements in Figs. S6(a, c). Therefore we see the effects of leakage currents and ion displacement currents in the hysteresis curves. Similar effects are seen in Fig. S7 below.

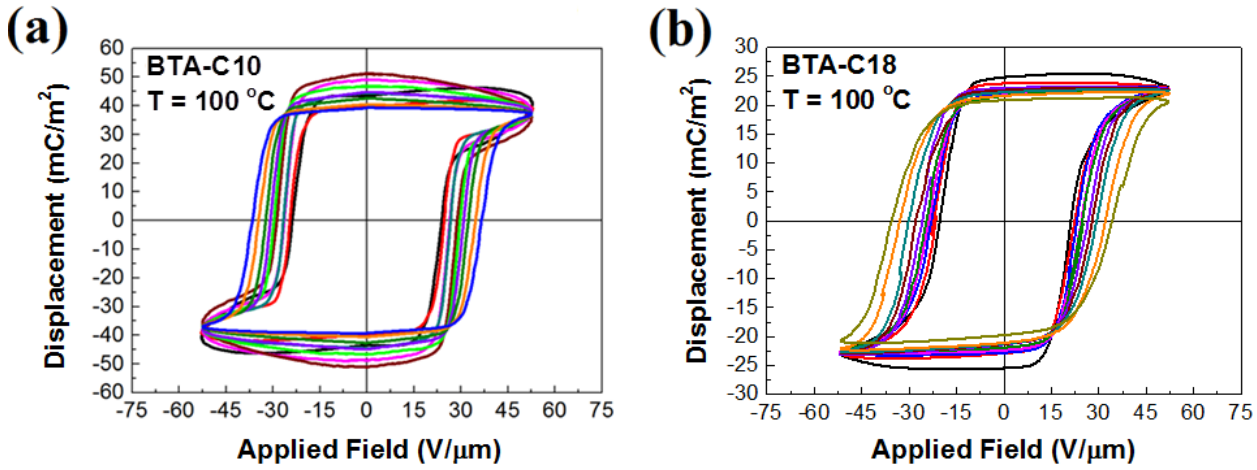

Fig. S7. Series of displacement charge *D* versus applied field *E* hysteresis loops measured in dynamic mode on Au/BTA-C10/Au (a) and Au/BTA-C18/Au (b) thin-film capacitors at different frequencies: 1 Hz, 5 Hz, 10 Hz, 15 Hz, 20 Hz, 30 Hz, 40 Hz, 50 Hz, 75 Hz, 100Hz and 0.5 Hz, 1 Hz, 3 Hz, 5 Hz, 15 Hz, 25 Hz, 35, 50 Hz, 75 Hz, 100Hz, respectively.

References

[1] C. F. C. Fitié, W. S. C. Roelofs, P. C. M. M. Magusin, M. Wübbenhorst, M. Kemerink, R. P. Sijbesma, *J. Phys. Chem. B* **2012**, *116*, 3928.

[2] M. Wübbenhorst, J. van Turnhout, *J. Non-Cryst. Solids* **2002**, *305*, 40.

[3] M. Serwadczak, M. Wübbenhorst, S. Kucharski, *J. Non-Cryst. Solids* **2007**, *353*, 4303.